eng

MDPI

Article

Phyto-Fabrication, Structural Characterization and Antibacterial Properties of *Hybanthus enneaspermus*-Assisted Mn-Doped ZnO Nanocomposites

Kanmani Kannan [1], Sankareswaran Muruganandham [1,*], Archana Ganeshan [2], Rajiv Periakaruppan [3,*], Nithish Kathiravan [3] and Sathyabama Narayanan [1]

[1] Department of Microbiology, Muthayammal College of Arts and Science (Autonomous), Rasipuram, Namakkal 637408, Tamil Nadu, India; kkanmanikavi@gmail.com (K.K.); nsathyabama1986@gmail.com (S.N.)
[2] Department of Biotechnology, PSGR Krishnammal College for Women, Coimbatore 641004, Tamil Nadu, India; archanag@psgrkcw.ac.in
[3] Department of Biotechnology, PSG College of Arts & Science, Coimbatore 641014, Tamil Nadu, India; nithishkathiravan123@gmail.com
* Correspondence: sankarsankar87@gmail.com (S.M.); rajivsmart15@gmail.com (R.P.)

Abstract: Green synthesis of nanocomposites offers an eco-friendly and viable solution to overcome the limitations of conventional chemical and physical methods as it uses biological agents to act as reducing and stabilizing agents. The current study's novelty is phyto-fabricated manganese (Mn)-doped zinc oxide (ZnO) nanocomposites using aqueous extract of *H. enneaspermus* by a biological method. Mn-doped ZnO nanocomposites were synthesized using manganese acetate and zinc acetate. The synthesized nanocomposites were characterized by XRD, FTIR, SEM, and EDX analysis. XRD shows the crystalline nature of nanocomposites with particle sizes of 30–40 nm, and FTIR reveals the presence of functional groups responsible for capping and stabilization. SEM analysis indicates spherical morphology with minor aggregation due to phytochemical interactions. EDX analysis of Mn-doped ZnO nanocomposites was used to verify the elemental composition, including Mn, Zn, O, and C. The anti-bacterial property of Mn-doped ZnO nanocomposites was assessed using the agar well-diffusion method against pathogens. The results of the anti-bacterial investigation proved that Mn-doped ZnO nanocomposites inhibit the growth of pathogens at different concentrations. The research concludes that the extract of *H. enneaspermus* acts as a capping and reducing agent in the synthesis process. The process can offer bio-compatible nanocomposites for new drug development against pathogens.

Keywords: *H. enneaspermus*; nanocomposites; Mn-doped ZnO; anti-bacterial activity

check for updates

Academic Editor: Masami Okamoto

Received: 12 December 2024
Revised: 17 January 2025
Accepted: 20 January 2025
Published: 21 January 2025

Citation: Kannan, K.; Muruganandham, S.; Ganeshan, A.; Periakaruppan, R.; Kathiravan, N.; Narayanan, S. Phyto-Fabrication, Structural Characterization and Antibacterial Properties of *Hybanthus enneaspermus*-Assisted Mn-Doped ZnO Nanocomposites. *Eng* **2025**, *6*, 21. https://doi.org/10.3390/eng6020021

Copyright: © 2025 by the authors. Licensee MDPI, Basel, Switzerland. This article is an open access article distributed under the terms and conditions of the Creative Commons Attribution (CC BY) license (https://creativecommons.org/licenses/by/4.0/).

1. Introduction

Nanotechnology is an emerging field of pharmaceutical sciences in which the size of materials is reduced to nanometers ranging around 1–100 nm. Currently, scientists are using various physical and chemical methods to synthesize these tiny particles [1]. Nowadays, most of the nanoscale materials are synthesized using chemical methods, but most of the methods might lead to negative impacts including environmental pollution, huge energy consumption, and health risks. To overcome these problems, an effective eco-friendly method called green synthesis was introduced [2]. Green synthesis refers to the production of nanoparticles using natural sources or processes that minimize the use of harmful chemicals and energy by utilizing plants, bacteria, or algae as reducing or stabilizing agents to convert the metal ions into nanoparticles [3]. It emphasizes sustainability,

cost-effectiveness, and biocompatibility. Green synthesized nanoparticles have diverse uses in various fields including biomedical applications [4], environment remediation [5], energy storage [6], fluorescent biological labeling [7], and so on. In the green synthesis methods, preparation of extracts usually involves leaves or any other part of the plant. In such extracts, phytochemicals act as reducing agents that make it easy to reduce the ions present in metals to nanoparticles. Such synthesis can also be controlled by various factors, including temperature, pH, metal ion concentrations, and reaction time, allowing further optimization for the size and morphology of nanoparticles. Characterization of green synthesized nanoparticles is also important to determine their properties and performance. UV–visible spectroscopy, FTIR, XRD, SEM, TEM, EDX, and Zeta potential were used to confirm the shape, size, and structural properties [8,9].

H. enneaspermus, commonly known as spade flower, is a tiny herb growing in the tropical regions of Africa, South Asia, and Australia. Being from the *Violaceae* family, it grows well on dry, rocky ground [10]. *H. enneaspermus* has medicinal values include aphrodisiac, antidiabetic [11], antiarthritic [12], antimicrobial [13], central nervous system [14], hypolipidemic [15], antiulcer and antisecretory [16], in vitro aldose reductase [17], and antiinfertile [18] properties. Traditional uses are supported by modern research indicating the wealth of bioactive compounds present, including tannins, flavonoids, alkaloids, saponins, and phenolic substances [19], which will eventually confirm the potential antimicrobial, antioxidant [20], and anti-inflammatory properties of the plant. This led to interest in its use in modern herbal medicines.

Various scientists have investigated the synthesis and characterization of Mn-doped ZnO nanocomposites. Hasan et al. [21] demonstrated the enhanced photocatalytic and antibacterial applications of Mn-doped ZnO synthesized through green methods when compared to traditional methods. Similarly, Djerdj et al. [22] (2007) characterized manganese oxide nanoparticles, and revealed their structural and magnetic properties, while Aadnan et al. [23] focused on the photocatalytic properties of Mn-doped ZnO in the degradation of azo dyes.

This study focused on the synthesis of Mn-doped ZnO nanocomposites with antibacterial properties using the aqueous extract of *H. enneaspermus* through the green chemistry method.

2. Materials and Methods

2.1. Preparation of H. enneaspermus Aqueous Extract

Healthy, young, and fresh *H. enneaspermus* was collected from the agricultural lands of Namakkal District, Tamil Nadu, India. The plant was washed with tap water followed by distilled water. A total of 10 g of the fresh plant was crushed into a paste using a mortar and pestle. Then, 100 mL of distilled water was added to the above paste and boiled at 80 °C for 10 min. The extract obtained was filtered with Whatman filter paper (No.1) and stored at −4 °C for further analysis [24].

2.2. Synthesis of Mn-Doped ZnO Nanocomposites

To prepare the Mn-doped ZnO nanocomposites, 0.1 M Manganese acetate and zinc acetate solutions were prepared separately and mixed in a ratio of 1:1 [21]. The solution was stirred continuously for 30 min using a magnetic stirrer. To that, 10 mL of the *H. enneaspermus* aqueous extract was added slowly while stirring it. pH 8 was maintained during the synthesis. The color change of the solution from pale yellow to white was observed, which confirmed the formation of the Mn-doped Zn nanocomposites [25]. The change in color of the solution was due to the activity of the phytochemicals present in the aqueous plant extract [26]. The pellet was obtained using centrifugation and dried in a hot

air oven to evaporate the moisture content. The dried pellet was then collected and stored in sterile containers for future studies.

2.3. Characterization of Mn-Doped ZnO Nanocomposites

The powdered Mn-doped ZnO nanocomposites were characterized using X-ray diffraction (XRD), Fourier Transform Infra-Red Spectroscopy (FTIR), Scanning Electron Microscope (SEM), and Energy Dispersive X-ray spectrophotometer (EDX). XRD was performed for the phase identification of Mn-doped ZnO nanocomposites. EDX was carried out to analyze whether the nanocomposites contain Mn, Zn, O, and C, [27] and SEM was used to analyze the shape and size of Mn-doped ZnO nanocomposites [28]. FTIR was used to check the capping agents on the surface of the nanocomposites [29].

2.4. Determination of Anti-Bacterial Properties

The anti-bacterial properties of Mn-doped ZnO composites synthesized using *H. enneaspermus* extract were evaluated against *Salmonella* sp. and *Bacillus subtilis* using the agar well diffusion method. Different concentrations (40 to 100 µg/mL) of *H. enneaspermus*-mediated Mn-doped ZnO composites were prepared and gentamycin was used as a positive control. The method with small modification was adapted to determine the anti-bacterial properties of Mn-doped ZnO nanocomposites [30]. Three replications were maintained. The results are expressed in terms of mean ± standard deviation.

3. Results and Discussion

3.1. XRD Analysis

The X-ray diffraction pattern determines the crystalline nature of the synthesized Mn-doped ZnO nanocomposites. Figure 1 describes the XRD pattern of *H. enneaspermus*-mediated Mn-doped ZnO nanocomposites and it reveals that the composites were crystalline with an average size of 30–40 nm, which was calculated by Scherrer's equation (JCPDS Card no. 00-001-1136). The XRD analysis of MnO_2 nanoparticles was carried out by Djerdj et al. [22], and they found a cubic structure and crystalline nature. Sagar Raut et al. [31] conducted research on the green synthesis of zinc oxide (ZnO) nanoparticles using *Ocimum tenuiflorum* leaves, and carried out XRD analysis. They demonstrated the formation of the wurtzite crystal structure of ZnO nanoparticles. XRD analysis of green synthesized *W. coagulans*-mediated Mn-doped ZnO nanocomposites was performed by Hasan et al. [21] and it shows clear peaks at 2θ = 31.7°, 34.3°, 36.1°, 47.2°, 56.4°, 60.7°, and 63.2°, corresponding to (100), (002), (101), (102), (110), (103), and (200).

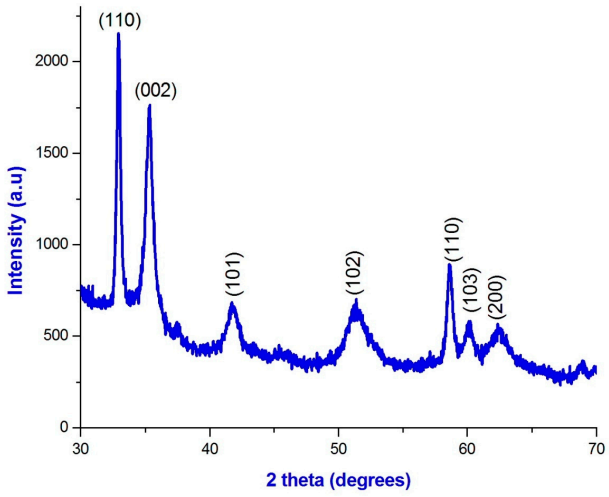


Figure 1. XRD analysis of *H. enneaspermus*-assisted Mn-doped ZnO nanocomposites.

3.2. FTIR Analysis

Fourier Transform Infrared (FTIR) Spectroscopy was essential to characterize the functional groups and chemical moiety of *H. enneaspermus*-mediated Mn-doped ZnO nanocomposites. Figure 2a illustrates the functional groups of *H. enneaspermus* extract (aqueous extract). The peaks at 3927, 3302, 2360, 1643, 694, 617, 601, 555, 462 and 416 cm^{-1} were obtained for an aqueous extract of *H. enneaspermus*, indicating the presence of O-H stretching of hydroxyl groups, =C-H stretching vibrations, C≡C or C≡N stretching vibrations, C-O stretching vibrations, and C-H bending of aromatic rings and alkyl halides. Figure 2b determines the occurrence of various peaks at 3934, 3819, 3765, 3078, 2368, 1126, 1026, 771, 663, 617, 601, 524, 493 and 416 cm^{-1}. It proves that the biomolecules shifted from the extract to the surface of nanocomposites. Moreover, the peaks from 771 to 416 cm^{-1} indicate the presence of metal oxide groups. Interestingly, the peaks at 416, 601, and 617 cm^{-1} were observed in both *H. enneaspermus*- and *H. enneaspermus*-mediated Mn-doped ZnO nanocomposites. Similarly, the FTIR spectra of Mn-doped ZnO nanocomposites were obtained by Aadnan et al. [23], showing a strong absorption peak in the region between 425 and 540 cm^{-1}. These peaks correspond to the infrared-active modes of wurtzite ZnO. Finally, the peaks at 1440 cm^{-1} and 1540 cm^{-1} correspond to the residual acetate groups due to the zinc acetate precursor.

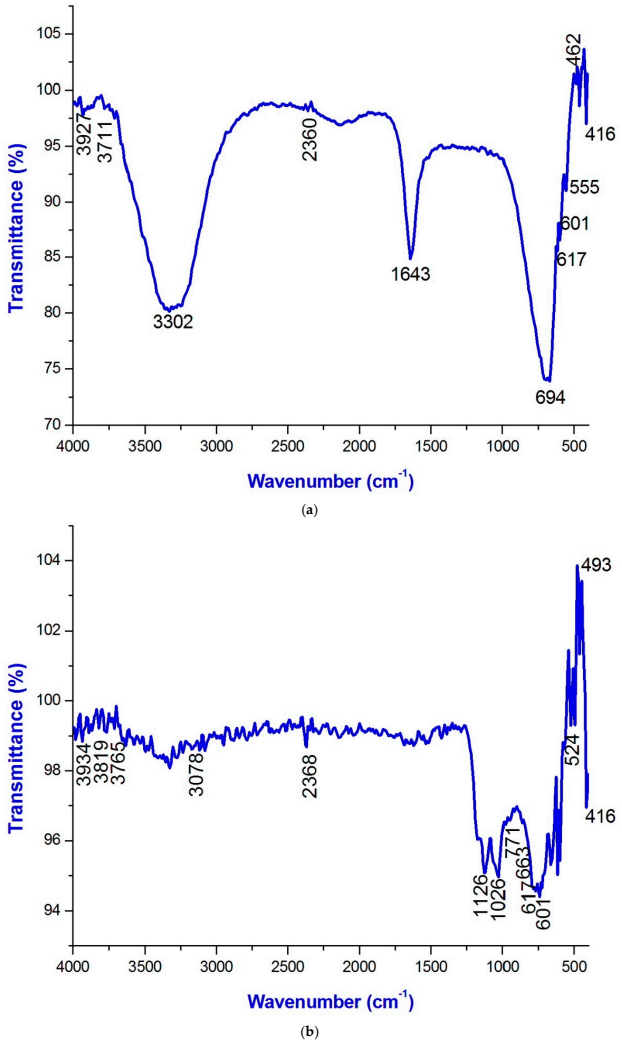


Figure 2. (**a**) FTIR analysis of *H. enneaspermus* aqueous extract. (**b**) FTIR analysis of *H. enneaspermus*-assisted Mn-doped ZnO nanocomposites.

3.3. SEM Analysis

SEM analysis was performed to study the surface morphology and size of the Mn-doped ZnO nanocomposites. Figure 3A,B displays well-dispersed and perfectly spherical Mn-doped ZnO nanocomposites. The surface was smooth, with a minor aggregation due to the interaction of phytochemicals from the aqueous *H. enneaspermus* extract. Spherical and polydispersity castor oil-mediated Mn-doped ZnO nanocomposites were produced by Khan et al. [32] and proved by SEM analysis. Vindhya et al. [33] synthesized spherical Mn-doped ZnO nanocomposites using *Annona muricata* leaf extract via a green chemistry approach.

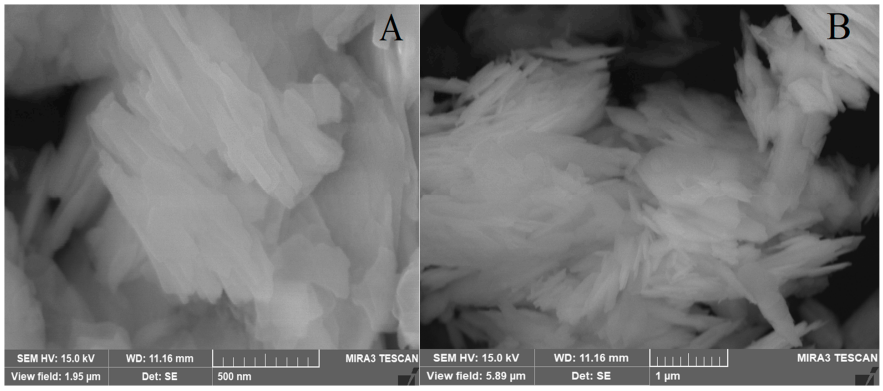


Figure 3. (**A**,**B**) SEM analysis of *H. enneaspermus*-assisted Mn-doped ZnO nanocomposites.

3.4. EDX Analysis

EDX analysis was performed to determine the elemental composition of *H. enneaspermus*-mediated Mn-doped ZnO nanocomposites. Figure 4 shows the presence of Mn, Zn, O, and C, which confirm the formation of the nanocomposites. The presence of carbon indicates the involvement of organic biomolecules from *H. enneaspermus* in biosynthesis as a reducing and capping agent. Similarly, Hasan et al. [21] reported the presence of oxygen, manganese, and zinc in the green synthesized Mn-doped ZnO nanocomposites through the EDX analysis.

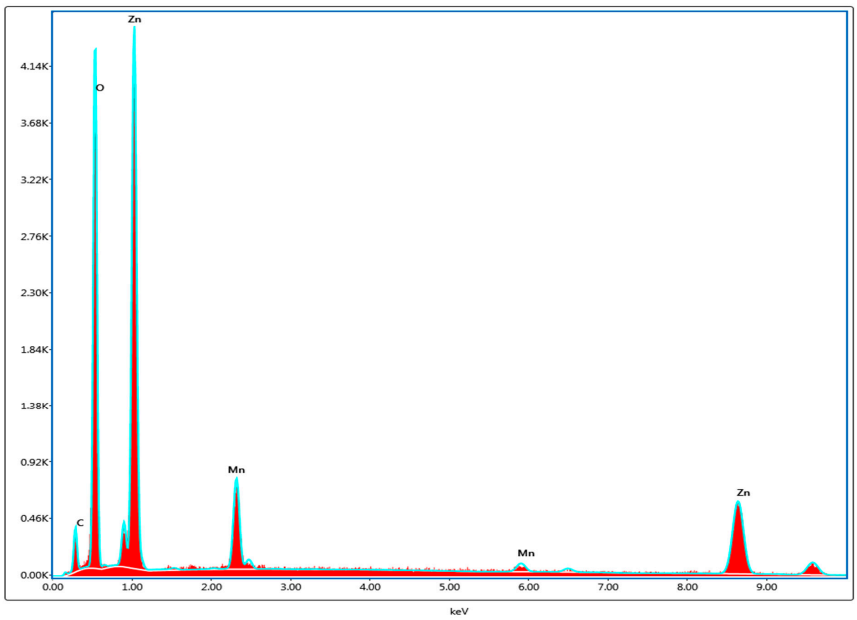


Figure 4. EDX analysis of *H. enneaspermus*-assisted Mn-Doped ZnO nanocomposites.

3.5. Determination of Anti-Bacterial Properties

The antibacterial activity test was conducted using *H. enneaspermus*-mediated Mn-doped ZnO nanocomposites against *Salmonella* sp. and *Bacillus subtilis*. The results of the antibacterial properties of Mn-doped ZnO nanocomposites are summarized in Table 1. Notably, at a concentration of 100 µg/mL, Mn-doped ZnO nanocomposites show the maximum zones of inhibition (14 mm) in *Salmonella* sp. as well as 21 mm for *Bacillus subtilis* (Figure 5a,b). Conversely, at a lower concentration of 40 µg/mL, Mn-doped ZnO nanocomposites display the minimum zones of inhibition for *Salmonella* sp. and *Bacillus subtilis*. Hasan et al. [21] found the anti-bacterial properties of *Withania* extract-mediated Mn-doped ZnO nanocomposites against *E. coli* and *S. aureus*. Canalli Bortolassi et al. [34] stated that Mn-doped ZnO nanocomposites disturb the cellular membrane by the interaction of metal ions with the bacterial cell membrane. It produces high amounts of reactive oxygen species that could lead to cell death [35].

Table 1. Determination of antibacterial properties of *H. enneaspermus*-assisted Mn-doped ZnO nanocomposites.

S.NO	Pathogens	Zone of Inhibition (Diameter in mm)				Gentamicin
		40 µg/mL	60 µg/mL	80 µg/mL	100 µg/mL	
1	*Bacillus subtilis*	10 ± 1	12 ± 1	18 ± 1	21 ± 1	11 ± 1
2	*Salmonella* sp.	6 ± 1	9 ± 1	11 ± 1	14 ± 1	6 ± 1

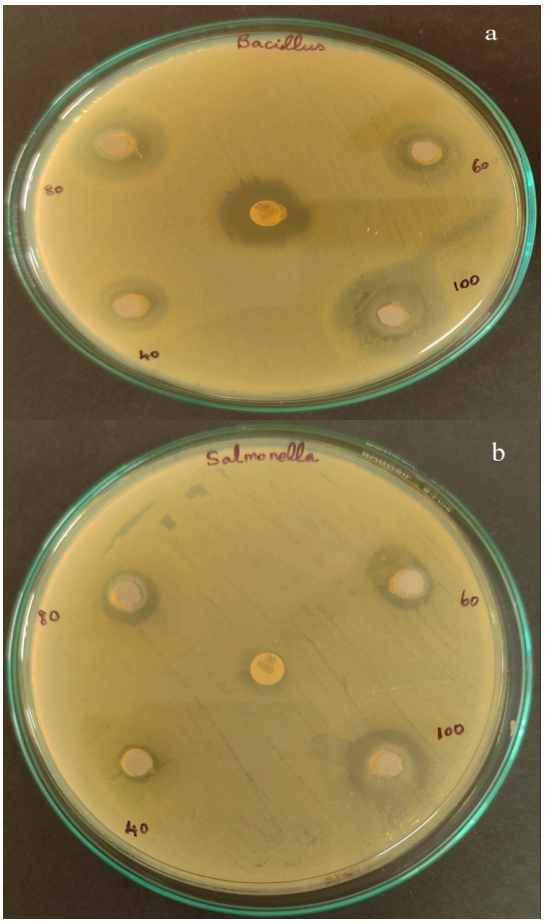


Figure 5. Antibacterial activity of *H. enneaspermus*-assisted Mn-doped ZnO nanocomposites: (**a**) *Bacillus subtilis*; (**b**) *Salmonella* sp.

4. Conclusions

Mn-doped ZnO nanocomposites were green synthesized using an aqueous extract of *H. enneaspermus* as effective reducing and capping agents. The characterization techniques, such as XRD, FTIR, SEM, and EDX, determine the crystalline nature of the synthesized nanocomposites and display the spherical morphology, with particle sizes of 30–40 nm. In addition, Mn-doped ZnO nanocomposites highly inhibit the growth of pathogens. This study emphasizes the role of *H. enneaspermus* as a biocompatible source in the synthesis of nanocomposites. Mn-doped ZnO nanocomposites may be utilized for developing new drugs in the medical field.

Author Contributions: Validation, R.P. and S.N.; Formal analysis, A.G., R.P. and N.K.; Investigation, K.K.; Data curation, A.G., N.K. and S.N.; Writing—original draft, K.K.; Writing—review & editing, S.M.; Project administration, S.M. All authors have read and agreed to the published version of the manuscript.

Funding: This research received no external funding.

Institutional Review Board Statement: Not applicable.

Informed Consent Statement: Not applicable.

Data Availability Statement: The original contributions presented in this study are included in the article. Further inquiries can be directed to the corresponding author.

Conflicts of Interest: The authors declare no conflict of interest.

References

1. Hussain, I.; Singh, N.B.; Singh, A.; Singh, H.; Singh, S.C. Green synthesis of nanoparticles and its potential application. *Biotechnol. Lett.* **2016**, *38*, 545–560. [CrossRef] [PubMed]
2. Ying, S.; Guan, Z.; Ofoegbu, P.C.; Clubb, P.; Rico, C.; He, F.; Hong, J. Green synthesis of nanoparticles: Current developments and limitations. *Environ. Technol. Innov.* **2022**, *26*, 102336. [CrossRef]
3. Disci-Zayed, D. Green Synthesis of Nanoparticles. Ph.D. Thesis, Universitätsbibliothek Kiel, Kiel, Germany, 2015.
4. Khan, Z.U.H.; Khan, A.; Chen, Y.; Shah, N.S.; Muhammad, N.; Khan, A.U.; Tahir, K.; Khan, F.U.; Murtaza, B.; Hassan, S.U.; et al. Biomedical applications of green synthesized Nobel metal nanoparticles. *J. Photochem. Photobiol. B Biol.* **2017**, *173*, 150–164. [CrossRef]
5. Akintelu, S.A.; Folorunso, A.S.; Folorunso, F.A.; Oyebamiji, A.K. Green synthesis of copper oxide nanoparticles for biomedical application and environmental remediation. *Heliyon* **2020**, *6*, e04508. [CrossRef]
6. Abuzeid, H.M.; Julien, C.M.; Zhu, L.; Hashem, A.M. Green synthesis of nanoparticles and their energy storage, environmental, and biomedical applications. *Crystals* **2023**, *13*, 1576. [CrossRef]
7. Bruchez, M., Jr.; Moronne, M.; Gin, P.; Weiss, S.; Alivisatos, A.P. Semiconductor nanocrystals as fluorescent biological labels. *Science* **1998**, *281*, 2013–2016. [CrossRef]
8. Fakhari, S.; Jamzad, M.; Kabiri Fard, H. Green synthesis of zinc oxide nanoparticles: A comparison. *Green Chem. Lett. Rev.* **2019**, *12*, 19–24. [CrossRef]
9. Slepička, P.; Slepičková Kasálková, N.; Siegel, J.; Kolská, Z.; Švorčík, V. Methods of gold and silver nanoparticles preparation. *Materials* **2019**, *13*, 1. [CrossRef] [PubMed]
10. Rajsekhar, P.B.; Bharani, R.A.; Angel, K.J.; Ramachandran, M.; Rajsekhar, S.P.V. *Hybanthus enneaspermus* (L.) F. Muell: A phytopharmacological review on herbal medicine. *J. Chem. Pharm. Res.* **2016**, *8*, 351–355.
11. Behera, S.; Mallick, B. Multi-elemental analysis of two anti-diabetic plant species: *Hemidesmus indicus* (L.) R. Br. and *Hybanthus enneaspermus* (L.) FV Muell and their callus cultures using EDXRF technique. *Inven. Rapid Pharm. Anal. Qual. Assur.* **2011**, *2*, 1–25.
12. Tripathy, S.; Sahoo, S.P.; Pradhan, D.; Sahoo, S.; Satapathy, D.K. Evaluation of anti arthritic potential of *Hybanthus enneaspermus*. *Afr. J. Pharm. Pharmacol.* **2009**, *3*, 611–614.
13. Retnam, K.R.; Britto, A. Antimicrobial activity of a medicinal plant *Hybanthus enneaspermus* (Linn.) F. Muell. *Indian J. Nat. Prod. Resour.* **2007**, *6*, 366–368.
14. Kar, D.M.; Maharana, L.; Rout, S.P. CNS activity of aerial parts of *Hybanthus enneaspermus* Mull. *Pharmacologyonline* **2010**, *3*, 959–981.

15. Satheesh Kumar, D.; Kottai Muthu, A. Evaluation of Hypolipidemic Activity of various extracts from whole plant of *Ionidium suffriticosum* (GING.) (family: Violaceae) in rat fed with high fat diet. *Int. J. Pharm. Pharm. Sci.* **2012**, *4*.
16. Sahoo, S.P.; Subudhi, B.B.; Ramchandran, S.; Dhanraju, M.D.; Kumaraswamy, B. Evaluation of anti-ulcer and anti-secretory activity of *Hybanthus enneaspermus*. *Int. J.* **2012**, *1*, 85–88.
17. Patel, D.K.; Kumar, R.; Kumar, M.; Sairam, K.; Hemalatha, S. Evaluation of in vitro aldose reductase inhibitory potential of different fraction of *Hybanthus enneaspermus* Linn F. Muell. *Asian Pac. J. Trop. Biomed.* **2012**, *2*, 134–139. [CrossRef] [PubMed]
18. Nathiya, S.; Senthamil Selvi, R. Anti-infertility effect of *Hybanthus enneaspermus* on endosulfan induced toxicity in male rats. *Int. J. Med. Biosci.* **2013**, *2*, 28–32.
19. Krishnamoorthy, B.S.; Nattuthurai, N.; Fathima, S. Phytochemical Study of *Hybanthus enneaspermus* (Linn.) F. Muell. *J. Pharmacogn. Phytochem.* **2014**, *3*, 6–7.
20. Adamolekun, M.M.; Akpor, O.A.; Adeola, O.E.; Ajinde, A.O.; Akpor, O.B. Phytochemical Analysis, Antioxidant and Antibacterial Activities of Aqueous Extract of *Hybanthus enneaspermus* Leaves. In Proceedings of the 2024 International Conference on Science, Engineering and Business for Driving Sustainable Development Goals (SEB4SDG), Omu-Aran, Nigeria, 2–4 April 2024; pp. 1–8.
21. Hasan, M.; Liu, Q.; Kanwal, A.; Tariq, T.; Mustafa, G.; Batool, S.; Ghorbanpour, M. A comparative study on green synthesis and characterization of Mn doped ZnO nanocomposite for antibacterial and photocatalytic applications. *Sci. Rep.* **2024**, *14*, 7528. [CrossRef]
22. Djerdj, I.; Arcon, D.; Jagličić, Z.; Niederberger, M. Nonaqueous synthesis of manganese oxide nanoparticles, structural characterization, and magnetic properties. *J. Phys. Chem. C* **2007**, *111*, 3614–3623. [CrossRef]
23. Aadnan, I.; Zegaoui, O.; El Mragui, A.; Daou, I.; Moussout, H.; Esteves da Silva, J.C. Structural, optical and photocatalytic properties of Mn Doped ZnO nanoparticles used as photocatalysts for Azo-dye degradation under visible light. *Catalysts* **2022**, *12*, 1382. [CrossRef]
24. Periakaruppan, R.; Naveen, V.; Danaraj, J. Green synthesis of magnesium oxide nanoparticles with antioxidant potential using the leaf extract of *Piper nigrum*. *JOM* **2022**, *74*, 4817–4822. [CrossRef]
25. Singh, H.; Desimone, M.F.; Pandya, S.; Jasani, S.; George, N.; Adnan, M.; Aldarhami, A.; Bazaid, A.S.; Alderhami, S.A. Revisiting the green synthesis of nanoparticles: Uncovering influences of plant extracts as reducing agents for enhanced synthesis efficiency and its biomedical applications. *Int. J. Nanomed.* **2023**, *18*, 4727–4750. [CrossRef]
26. Alamdari, S.; Sasani Ghamsari, M.; Lee, C.; Han, W.; Park, H.H.; Tafreshi, M.J.; Afarideh, H.; Ara, M.H.M. Preparation and characterization of zinc oxide nanoparticles using leaf extract of *Sambucus ebulus*. *Appl. Sci.* **2020**, *10*, 3620. [CrossRef]
27. Kumar, S.S.; Venkateswarlu, P.; Rao, V.R.; Rao, G.N. Synthesis, characterization and optical properties of zinc oxide nanoparticles. *Int. Nano Lett.* **2013**, *3*, 30. [CrossRef]
28. Mohan, A.C.; Renjanadevi, B.J.P.T. Preparation of zinc oxide nanoparticles and its characterization using scanning electron microscopy (SEM) and X-ray diffraction (XRD). *Procedia Technol.* **2016**, *24*, 761–766. [CrossRef]
29. Eid, M.M. Characterization of Nanoparticles by FTIR and FTIR-Microscopy. In *Handbook of Consumer Nanoproducts*; Springer: Singapore, 2022; pp. 1–30.
30. Narendhran, S.; Rajiv, P.; Sivaraj, R. Toxicity of ZnO nanoparticles on germinating *Sesamum indicum* (Co-1) and their antibacterial activity. *Bull. Mater. Sci.* **2016**, *39*, 415–421. [CrossRef]
31. Sagar Raut, D.P.; Thorat, R. Green synthesis of zinc oxide (ZnO) nanoparticles using *Ocimum tenuiflorum* leaves. *Int. J. Sci. Res* **2015**, *4*, 1225–1228.
32. Khan, S.B.; Khan, M.I.; Nisar, J. Microwave-assisted green synthesis of pure and Mn-doped ZnO nanocomposites: In vitro antibacterial assay and photodegradation of methylene blue. *Front. Mater.* **2022**, *8*, 710155. [CrossRef]
33. Vindhya, P.S.; Kunjikannan, R.; Kavitha, V.T. Photocatalytic and antimicrobial activities of pure and Mn doped ZnO nanoparticles synthesised by *Annona muricata* leaf extract. *Int. J. Environ. Anal. Chem.* **2024**, *104*, 5083–5098.
34. Canalli Bortolassi, A.C.; Guerra, V.G.; Aguiar, M.L.; Soussan, L.; Cornu, D.; Miele, P.; Bechelany, M. Composites based on nanoparticle and pan electrospun nanofiber membranes for air filtration and bacterial removal. *Nanomaterials* **2019**, *9*, 1740. [CrossRef] [PubMed]
35. Al-Musawi, M.H.; Ibrahim, K.M.; Albukhaty, S. In vitro study of antioxidant, antibacterial, and cytotoxicity properties of *Cordia myxa* fruit extract. *Iran. J. Microbiol.* **2022**, *14*, 97–103. [CrossRef] [PubMed]

Disclaimer/Publisher's Note: The statements, opinions and data contained in all publications are solely those of the individual author(s) and contributor(s) and not of MDPI and/or the editor(s). MDPI and/or the editor(s) disclaim responsibility for any injury to people or property resulting from any ideas, methods, instructions or products referred to in the content.